PENA TEKNIK
JURNAL ILMIAH ILMU - ILMU TEKNIK

Vol. 8, No.1, Maret (2023)
p-ISSN 2502-8952
e-ISSN 2623-2197
https://ojs.unanda.ac.id/index.php/jiit/index

Metoda GTAW Welding Joint Strength Study for AISI 1045 Application of Milling Tools

[1] Toto Triantoro B W, [2] Waluyo M B

[1]Department of Mechanical Engineering, Faculty of Manufacturing Engineering, Universitas Jenderal Achmad Yani
[2]Bandung State Polytechnic Mechanical Engineering Department
E-mail: [1]trians65@yahoo.co.id, [2] waluyomb@gmail.com

Keywords:

GTAW Welding: AISI 1045 Steel: Mechanical Properties.

Abstract

Welding is a permanent connection process for metal materials using heat energy. The GTAW (Gas Tungsten Arc Welding) welding method is carried out on AISI 1045 steel material with a solid round shape, which has the characteristics and properties of the material slightly above low carbon steel. The welding process was carried out based on AWS A5.18 standard specifications in this study. by varying the welding amperage between ±70, ±90, and ±110 amperes as well as the ER70S-G series electrodes. To check the welding results with the amperage variation, perform tensile testing with standard ASTM A-370 testing, hardness testing using the Vickers method with standard ASTM E-92 testing, microstructure inspection, and grain size calculations as a control for the results of the hardness test. The focus of testing and inspection is carried out in three influential areas, namely, areas of weld metal, HAZ (Heat Affected Zone), and base metal. The results of this study show that for ±70 A welding amperage, the tensile test results in all samples breaking in the weld metal area. While welding amperage ±90A broke two samples in the weld metal area, welding amperage ±110A broke one sample in the weld metal area. For the hardness test results at ±110 A amperes, the hardness ratio in the weld metal area to the HAZ area shows that the difference in hardness is not too large compared to the two amperes used, so a welding amperage of ±110 A can be recommended. The microstructure test showed that most of the weld metal was pearlite and martensite, with a small amount of bainite. The hardness test showed that the weld metal was harder than the HAZ area and the base metal. Likewise, the results of grain size calculations using the Heyn method for regions with higher hardness make the grain sizes appear denser and smaller.

1. INTRODUCTION

One of the crucial production paths for most industrial businesses is welding as a fabrication technique. Welding is one of the primary manufacturing processes (Rudrapati, 2022). The selection of a welding technique depends on several parameters for a given application (Kumar & Singh, 2019). According to DIN (Deutsche Industrie Norman), welding is a metallurgical bond at a metal or alloy metal joint carried out in a melted or liquid state (Aditia et al., 2019). In other words, welding is a local, permanent connection of several metal rods using heat energy (Wiryosumarto in (Hardiyanto, 2020)). The GTAW welding method is a welding process that uses an arc between non-consumable tungsten electrodes at the welding point (Al Huda, 2019). The definition of welding, according to the American Welding Society (Pangaribowo & Putra, 2019), is a metal or non-metallic joining process that is carried out by heating the material to be joined to the melting temperature, which is carried out with or without using pressure or with or without using filler metal. According to Lawrence in (Anhar, 2019), welding is a metal joining process.

The welding process has many factors that affect the quality of the results, including the welding machine used, the materials used, the welding procedure, the welding method, the welding current, and the welder. This welding process is well-suited for fragile metals, making it possible to obtain high-quality welds (Dharma et al., 2022). This process uses argon shielding gas with or without applying pressure (Haikal et al., 2021). This process can be used with or without the addition of filler metal. The GTAW method is indispensable as a tool for many industries because it produces high-quality welding results with relatively low operating costs compared to other methods in its class (Li et al., 2021). In this study, the material used was AISI 1045 steel, namely carbon steel. Carbon steel has more substantial mechanical properties and is widely used as a machining tool because it has a relatively large carbon content of ±0.45%, a higher hardness level than low-

carbon steel (Purnomo et al., 2019). This research is intended for application to milling machine tools. Solid round samples with a diameter of 20 mm were chosen to approach the standard shape of milling tools. The results of this study can be used to join together two different materials or high-strength materials (Junaidi et al., 2022).

Gultom & Sabri's (2021) research showed that the average Brinell hardness test results for the mechanical properties of AISI 1045 steel for SMAW welding in the welding area with E-6013 electrodes at a current of 100 A was 160.04 BHN. For GTAW welding with TG-filer S50 at a current of 100 A, it was 172.53 BHN. The average value of SMAW welding voltage with an E-6013 electrode at 100 A current is 323.14 MPa, and that of GTAW welding with a TG-S50 filler at 100 A current is 411.57 MPa. The shape of the microstructure in the weld area with GTAW welding has a smaller microstructure than SMAW welding; this shows that the hardness value in the GTAW weld area is greater than the hardness value in the SMAW weld area. For fragile metals, we are making it possible to obtain high-quality welds.

Meanwhile, according to research conducted by Purnama (2022), SMAW welding has a greater tensile strength than GTAW welding. SMAW welding has the highest tensile strength of 52.43 Kgf/mm2 and the lowest tensile strength of 31.22 Kgf/mm2. At the same time, GTAW welding has the highest tensile strength of 31.88 Kgf/mm2 and the most insufficient tensile strength of 18.84 Kgf/mm2. Based on the findings of microstructural analysis by Banjarnahor (2019), microstructural analysis shows that specimens without welds have ferrite and pearlite microstructures, welded areas have cementite microstructures, and HAZ areas have bigger ferrite and pearlite microstructures. The Solidworks simulation's joint strength is 698 MPa with a tensile force of 36000 N.

Based on the background above, this study's formulation of the problem is to get the proper welding amperage for AISI 1045 steel using the GTAW method based on AWS A5.18 standard welding specifications. Mechanical properties are tested and inspected due to variations in the amperage of the welding performed (Kumar & Singh, 2019). The research aimed to find the proper welding amperage based on the AWS A5.18 standard for joining worn milling tools (Wardani et al., 2020). Scope of the problem the material used as the workpiece is AISI 1045 steel with a carbon content between (0.3 - 0.6%) with a solid sample form Ø=20 mm in diameter with AWS A5.18 standard welding specifications using amperage variations between (±70 - ±110) Amperes.

2. METHODS

The research method used experimental and observation techniques. The empirical research method is used to find the effect of specific treatments (Sugiyono, 2019). Exploratory research is one method that uses a quantitative approach (Sari et al., 2022). This research was carried out with the preparation of materials and equipment adapted to field conditions. The AISI 1045 material with a diameter of 20 mm as a sample was cut to a length of 220 mm based on the tensile test standard, ASTM A-370, as shown in Figure 1.

Furthermore, all the tensile samples were cut using a cutting machine into two parts. The next step is making a weld seam with a single V shape on both parts to be connected (see figure 3. Next, the welding process was carried out using the GTAW method with amperage variations of ±70, ±90, and ±110 based on the AWS A5.18 standard, after that the removing capping process was carried out using a lathe of result welding below figure 4.

Before the tensile test, the welding results are checked for NDT (Non-Destructive Tests) using the dye-penetrant method in figure 5. From the tensile test results, only samples that break off in the base metal area will be examined and tested. Three regions have an impact on the results of the welding, namely: the weld metal area, HAZ, and base metal area (Hammi et al., 2021). and then to be observed and analyzed as a recommendation for welding on materials with high strength or combining materials with different types.

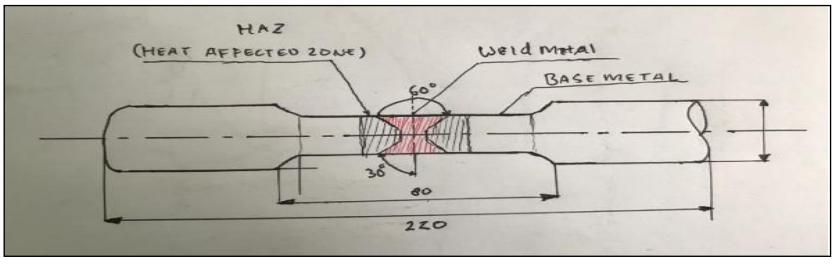

Figure 1 Research sample planning.

Tensile testing is one of the mechanical tests that aim to determine the mechanical properties of a metal, namely, among others, tensile strength, yield strength, and strain (Mahalle et al., 2019). The highest tensile strength refers to the quality of the weld (Bukhori, 2021). Then the test results are analyzed using a flowchart, as shown in Figure 2. This research is planned to facilitate the stages of the research process that will be carried out. The welding amperage is independent, while the fixed variable is the AWS A5.18 standard (Sayed et al., 2019).

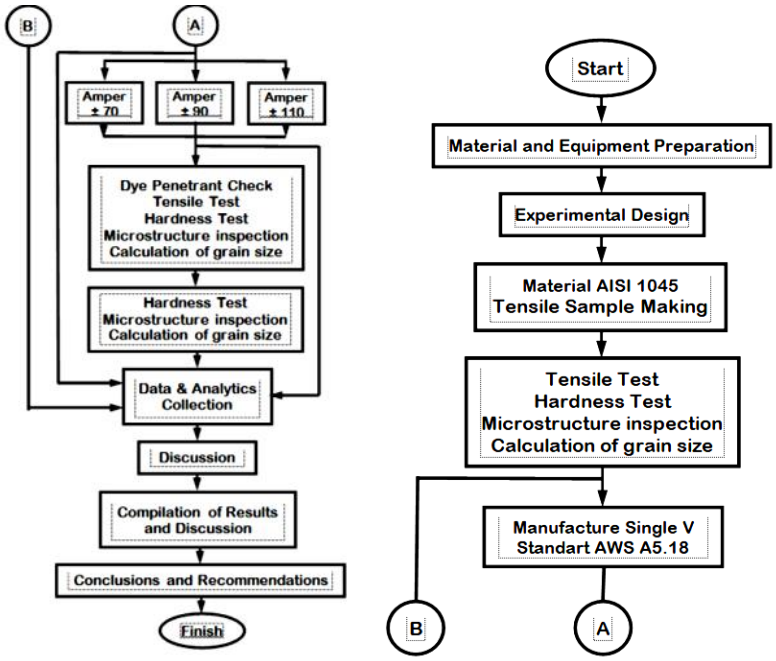

Figure 2 Research flow chart

3. RESULT AND DISCUSSION

After the cutting process is carried out according to the length and size required, the next step is to make welding seams by turning the seam angle to 60°, as shown in Figure 3 below.

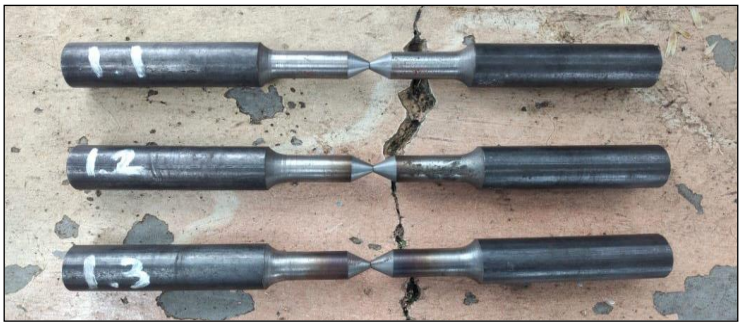

Figure 3 The results of turning the sample from a single V

The welding process is carried out with a sample size of Ø:20 mm in diameter and 220 mm in length, according to the standard size of the tensile test, where the welding process is carried out in three layers. After the welding process is carried out, the next step is to remove the welding capping utilizing the turning process, as shown in Figure 4 below.

Figure 4 Results of welding and turning processes.

The next step is to carry out a non-destructive inspection (NDI) process, which is carried out using the dye-penetrant method. This inspection will provide information regarding the presence of cracks visually after the welding process and the removal of weld chips.

Figure 5 Results of dye-penetrant inspection

The dye-penetrant inspection of the welding process results showed that for the welding amperage of ±70 amperes, many red spots appeared on the three samples, as shown in Figure 5b. This indicates that the welding process using ±70 amperes resulted in many defects. Whereas for welding at ±90 amperes, there were several red spots visible in one sample, for welding at ±110 amperes, it showed very few red spots visible in all samples, so the defects that occurred for welding at ±110 amperes were quite good.

Table 1. Tensile test data from welding AISI 1045 materials

No	Sample	Ultimate Tensile Strength (Mpa)	Tensile Stress Yield (Ofseet 2%) (Kgf/mm2)	Maximum Load (KN)	Information
	Raw Material Amper ±70	707,20	680,27	68,64	
1	Sample 1.1	316,22	288,52	39,869	Break up in welded metal
2	Sample 1.2	365,90	311,91	46,351	Break up in welded metal
3	Sample 1.3	248,16	297,11	45,292	Break up in welded metal
	Rata-rata	310,09	229,18	43,837	
	Standart Deviasi	48,25	70,64	2,84	

	Amper ±90				
1	Sample 2.1	596,76	458,38	80,187	Break up in welded metal
2	Sample 2.2	607,74	489,15	76,502	Break up in base metal
3	Sample 2.3	354,72	263,70	45,218	Break up in welded metal
	Rata-rata	519,74	405,74	67,300	
	Standart Deviasi	202,25	299,90	15,69	
	Amper ±110				
1	Sample 3.1	576,00	494,07	78,824	Break up in base metal
2	Sample 3.2	600,51	518,73	74,166	Break up in welded metal
3	Sample 3.3	615,42	555,15	82,821	Break up in base metal
	Rata-rata	797,31	522,65	78,600	
	Standart Deviasi	159,91	25,09	3,54	

At ±70 A amperage, an average tensile stress of 229.18 N/mm^2 was obtained, and all samples broke in the weld metal area. While welding at a current of ±90 A, it got a moderate tensile stress of 405.07 N/mm^2. In sample 2.2, it broke in the base metal area, and the average tensile stress in welding amperes of ±110 A was 522.65 N/mm^2. Two samples broke in the base metal area, namely samples 3.1 and 3.3, where the average tensile stress with amperage ±110 A is the greatest compared to the other two types of amperage.

Figure 6 Sample evidence of tensile test results

Figure 6 above shows the sample results from the tensile test that has been carried out. For a welding amperage of ±110A, two samples break off in the base metal region. This welding amperage can be a reference for the welding.

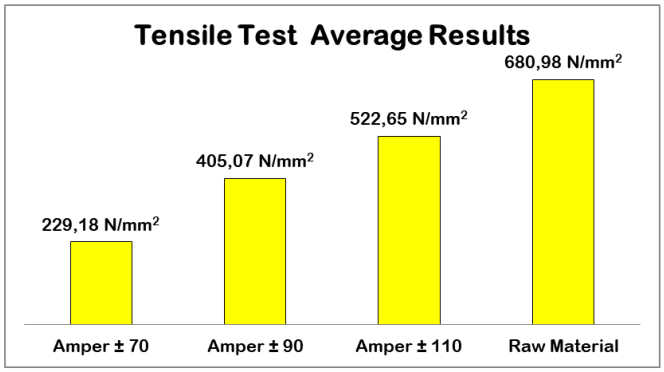

Figure 7 Comparison graph of tensile test results

The hardness graph below shows that the highest average hardness value in the weld metal area is ampere ±110A, with a hardness value of 268.13 HV. The most important thing from this hardness result is the hardness comparison between the weld metal area of 226.13 HV, the HAZ of 227.22 HV, and the base metal of 225.45 HV, and this ratio is not too big. So that the two samples broke up in the base metal region. Meanwhile, at ±90A welding amperage, the difference in hardness between the weld metal area and the HAZ is significant enough that one sample breaks off in the base metal area (Sugestian, 2019). The weld was not tested for hardness while welding at ±70A ampere because three samples broke in the weld metal area.

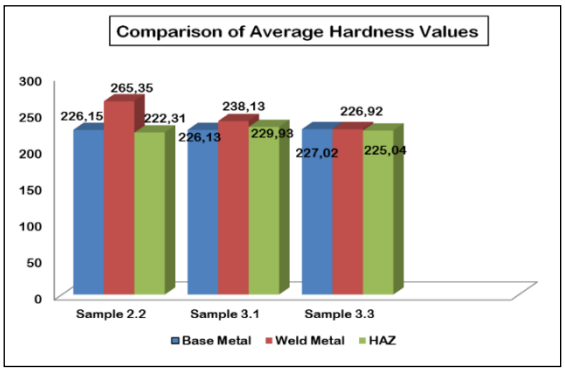

Figure 8 Graph of hardness test comparison

There is no significant difference in hardness in the base metal area for all samples. This is because the AISI 1045 material consists of a ferrite structure, which is white or light in color, while the pearlite structure, which looks dark, is grey. This is because there are no significant microstructural changes in this area. After all, it is not affected by the effects of heat caused by welding. The influence of the heat effect is concentrated in the weld metal area and the HAZ area for materials with a carbon content of around 0.46%, so this material is quite complicated. As shown in Figure 9, the obtained microstructure shows a boundary between the base metal and the weld metal, which have different surface shapes.

From the microstructure data obtained, the grain size can be calculated. By using the Hyne method equation, as in the formula below,

$$Dm = \frac{L.p.10^3}{Z.V}(\mu m) \quad (1)$$

Note: The length of the line is 60mm
P: Number of lines 6
Z: The number of truncated grains
V: Enlargement of microstructure

This grain size is calculated as a comparison control for the hardness value in each welding area, with the welding amperage variation as the independent variable. Meanwhile, the microstructure obtained was only in samples that broke off in the base metal area, namely when welding at amperes of ±90 and ±110A.

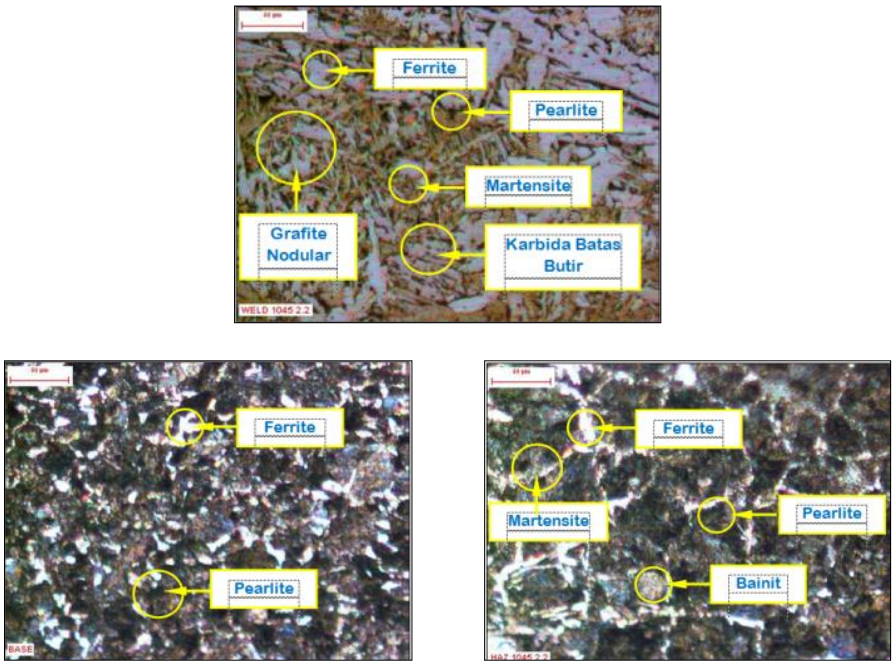

Figure 9 Microstructure of ±90 ampere welding results

The phases that appear in the base metal area at ±90 A welding amperage with 500x magnification are the white ferrite phase, which merges with the dark black pearlite phase, which collects with a large enough area to combine with the ratio of ferrite seen to be less than pearlite, which is more numerous around 60% for steel with a carbon content of around 0.46%. Whereas in the HAZ area, the white ferrite phase looks much reduced, while the dark black pearlite also begins to decrease and gather to enlarge. This is due to the influence of heat. There is a slight martensite phase that appears due to the effect of heat caused by the welding process, and this phase is sharp and rough in shape, and there is a tiny bit of bainite phase, which is in the form of a soft round shape. A slight pearlite phase remains visible for the weld metal area, while the ferrite phase changes to a nodular graphite phase. While the martensite phase is present in sufficient quantities and a small carbide phase is current, this area is more complex than the base metal and HAZ regions.

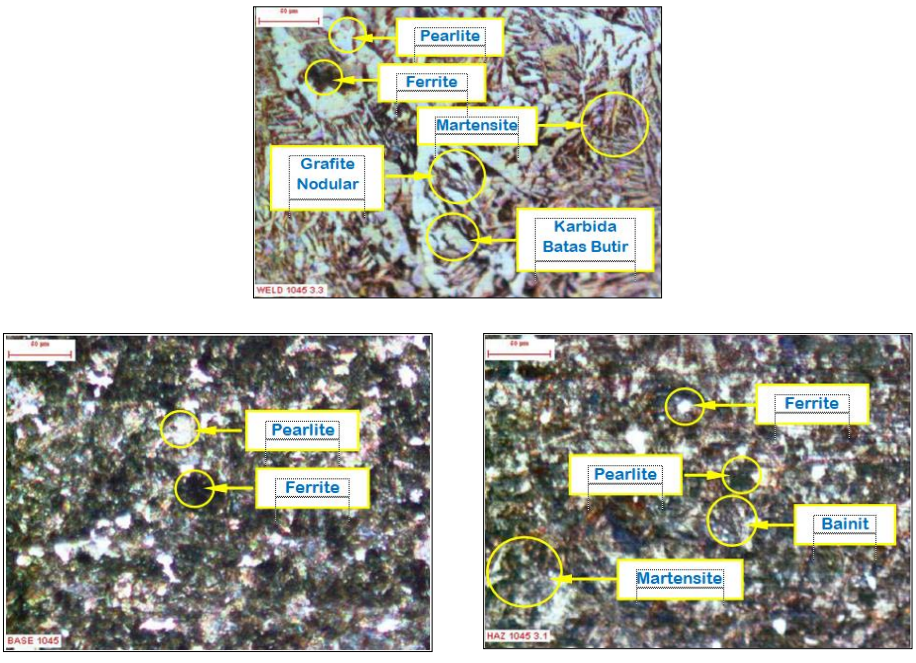

Figure 10 Microstructure of ±110 ampere welding results

In the base metal area for ±110 A welding amperage with 500x magnification, a white ferrite phase is still seen much less with increasing welding current. Meanwhile, the dark black pearlite phase blends quite nicely with ferrite, which appears less and less than pearlite, which has a higher concentration. In the HAZ region, the white ferrite phase seems much reduced compared to the base metal area, while the dark black pearlite phase in this area is much reduced. While the martensite phase occurs as a result of the effect of heat caused by the increase in the amperage of the welding process being carried out, this phase has a sharp shape, and there is much less of the bainite phase, which has a soft round shape with increasing welding current. There is still less pearlite phase in the weld metal area, while the ferrite phase has changed to a nodular graphite phase. Meanwhile, the martensite phase is much more abundant with increasing welding current, and there is less grain boundary carbide phase, so this area is more complex than the base metal and HAZ areas (Moghaddam & Kolahan, 2021). The hardness value results from the hardening process, transforming the soft ferrite or austenite microstructure into a complex martensite structure (Saputra, 2020).

Table 2 Calculation of grain size

No	Sample	Zone	Z value	Item size value
1	±70 A	*Base metal*	3300	109,1 µm
2		HAZ	2500	144 µm
3		*Weld metal*	5600	64,2 µm
1	±90 A	*Base metal*	3700	97,3 µm
2		HAZ	3300	110 µm
3		*Weld metal*	5200	70 µm
1	±110 A	*Base metal*	3400	105 µm
2		HAZ	2700	133,3 µm
3		*Weld metal*	5200	69 µm

The results of the grain size calculation shown in Table 2 above show that the smaller the grain size, the more complex the rock in that area. This explains that the hardness test results are correct because an error in attaching the hardness testing penetrator to the workpiece will result in inaccurate hardness calculation results.

4. CONCLUSIONS

Based on the examination of the chemical composition of AISI 1045 steel, medium carbon steel has a carbon content of around 0.46%, while the standard carbon content is in the range (of 0.25% - 0.60%). From the welding amperage tensile test results of ±110A, the average tensile strength was around 55.265 N/mm^2, one sample broke in the weld metal area, and two samples broke in the base metal area. This explains that large welding amperes can be recommended for welding with high-strength steel materials for welding AISI 1045 steel with the GTAW method based on the AWS A5.18 standard. While the average tensile strength for welding using high welding amperes approaches the raw material tensile strength of 68,098 N/mm^2.

The Vickers method was used to test the hardness from the results of welding AISI 1045 material in three welding areas, including; the area of weld metal, HAZ, and base metal. Amperage ±70A is not carried out for welding because all samples break in the weld metal area, so this amperage is not recommended. The welding amperage of ±90A in sample 2.2 breaks in the base metal so that this sample can be tested for hardness. For the weld metal area, the hardness is 265.35 HV, while for the HAZ area, the hardness is 222.32 HV for the base metal area, 226.15 HV. Meanwhile, the difference in hardness between the weld metal area and the HAZ area is around 43 HV. For the welding amperage of ±110A for sample 3.1, the hardness value of the weld metal is 238.13 HV, while in the HAZ area, the hardness value is 229.93 HV and the base metal is 226.13 HV so that the hardness difference between the weld metal area and the HAZ area is 8.2 HV. Whereas in sample 3.3, the hardness value of the weld metal was 226.67 HV, while in the HAZ area, the hardness was around 225.04 HV, this difference was not significant, around 1.6 HV, while in the base metal area, it was 227.02 HV.

The difference in hardness between the weld metal area and the HAZ area should be more negligible, the slightest difference is better, and it is possible to break in the base metal area.

With a magnification of 500x, it can be seen that the white ferrite phase and the dense black pearlite phase gather with a large enough area to blend with a smaller ferrite ratio compared to thicker pearlite, which is around 60% in the base metal region. The ferrite and pearlite phases are reduced for the HAZ region, and the aggregate is enlarged. This area contains a small amount of martensite due to the heat from the welding process, and this phase has a rough, sharp shape and a small amount of soft, rounded bainite. A slight pearlite phase remains visible for the weld metal area, while the ferrite phase changes to a nodular graphite phase. While the martensitic phase is appreciable and a small carbide phase is present, this region is more complex than the base metal region. In this study, based on the results of the tests carried out, current variations affect the welding process's tensile strength, hardness, and microstructure. The use of high amperage in this welding can be recommended, especially for welding the combination of different materials, such as welding between HSS (High-Speed Steel) and AISI 1045, for further research. Grain size calculations were carried out using the Heyn method from the microstructure taken from the welding results as a control for hardness testing. The grain size calculations show that the hardness results are significant, especially in the area of weld metal, where the grain size is getting smaller. The hardness data and grain size calculations are appropriate.

5. ACKNOWLEDGMENTS

Thank you to all parties who have played a role from the research stage to the publication stage of this research journal.

6. REFERENCES

Aditia, A., Nurdin, N., & Ismy, A. S. (2019). Analisa kekuatan sambungan material AISI 1050 dengan ASTM A36 dengan variasi arus pada proses pengelasan SMAW. *Journal of Welding Technology*, *1*(1), 1–4.

Al Huda, M. (2019). Penentuan Parameter Proses Pengelasan Yang Tepat Untuk Menghilangkan Cacat Linear Indication Pada Produk Gate Valve. *Jurnal Teknologika*, *9*(2).

Anhar, M. (2019). Pendinginan Pengelasan dengan Metode SMAW pada Kekerasan Baja Karbon ST37 dengan Media Serbuk Semen Abu-Abu pada Beban Rockwell 100 kgf. *ROTASI*, *21*(3), 140–146.

Banjarnahor, F. (2019). *Studi Pengelasan Tig (Tungsten Inert Gas) Terhadap Kekuatan Sambungan Dan Sifat Mekanik Pada Baja Aisi 1045*. Universitas Sumatera Utara.

Bukhori, S. (2021). *Analisa Pengaruh Arus Pengelasan Resistance Spot Welding Terhadapat Sifat Mekanis Dan Struktur Mikro Material Plat Galvanil*. Institut Teknologi Indonesia.

Dharma, S., Suherman, S., Sarjianto, S., Sebayang, R., & Kurniyanto, H. B. (2022). Pengaruh Kuat Arus terhadap Sifat Mekanis pada Aluminium Al-Si-Fe dengan Filler Er 4043 Metode Pengelasan GTAW. *Jurnal Rekayasa Mesin*, *17*(1), 103–112.

Gultom, R. R. F., & Sabri, M. (2021). Analisa Sifat Mekanik Dan Struktur Mikro Terhadap Pengelasan Baja Aisi 1045 Dengan Metode SMAW Dan GTAW Pada Arus 100 Ampere. *DINAMIS*, *9*(2), 7.

Haikal, H., Chamim, M., Andriyansyah, D., Wiyono, A., Baskoro, A. S., & Isnarno, I. (2021). Peningkatan Kedalaman Penetrasi Las Stainless Steel 304 dengan Medan Magnet Eksternal pada Pengelasan Autogenous Tungsten Inert Gas Welding. *Jurnal Rekayasa Mesin*, *12*(1), 87–94.

Hammi, M., Ziat, Y., Zarhri, Z., Laghlimi, C., & Moutcine, A. (2021). Epoxy/alumina composite coating on welded steel 316L with excellent wear and anticorrosion properties. *Scientific Reports*, *11*(1), 12928.

Hardiyanto, S. (2020). Optimalisasi Proyek Pembangunan Gedung Parkir Dan Masjid RSUD Pare Oleh PT Arwi Graha Sejahtera Dengan Metode Jalur Kritis (Critical Path Method). *Jurnal Simki Unp*, *01*, 1–13.

Junaidi, A. K., Machdalena, M., Weriono, W., Hariman, H., & Firdaus, M. (2022). The Effect of GTAW Welding Current on the Strength of AISI Steel 1045. *Journal of Ocean, Mechanical and Aerospace-Science and Engineering-*, *66*(1), 32–35.

Kumar, S., & Singh, R. (2019). Optimization of process parameters of metal inert gas welding with preheating on AISI 1018 mild steel using grey based Taguchi method. *Measurement*, *148*, 106924.

Li, Y., Su, C., & Zhu, J. (2021). Comprehensive review of wire arc additive manufacturing: Hardware system, physical process, monitoring, property characterization, application and future prospects. *Results in Engineering*, 100330.

Mahalle, G., Salunke, O., Kotkunde, N., Gupta, A. K., & Singh, S. K. (2019). Neural network modeling for anisotropic mechanical properties and work hardening behavior of Inconel 718 alloy at elevated temperatures. *Journal of Materials Research and Technology*, *8*(2), 2130–2140.

Moghaddam, M. A., & Kolahan, F. (2021). *Activated Gas Tungsten Arc Welding Process Optimization Using Artificial Neural Network and Heuristic Algorithms*.

Pangaribowo, B. H., & Putra, W. H. A. (2019). Studi Pengaruh Pemanasan Awal pada Pengelasan Ulang Baja ASTM A36 akibat Reparasi terhadap Sifat Mekanis menggunakan Proses Las FCAW. *Jurnal Teknik ITS*, *7*(2), G150–G155.

Purnama, A. (2022). Kajian Eksperimental Perbandingan Hasil Pengelasan Model Smaw Dan Gtaw Terhadap Kekuatan Tarik Material Baja St 37. *Jurnal Ilmiah Mahasiswa Teknik [JIMT]*, *2*(5).

Purnomo, D. J., Jokosisworo, S., & Budiarto, U. (2019). Analisa Pengaruh Holding Time Tempering Terhadap Kekerasan, Keuletan, Ketangguhan dan Struktur Mikro Pada Baja ST 70. *Jurnal Teknik Perkapalan*, *7*(1).

Rudrapati, R. (2022). Effects of welding process conditions on friction stir welding of polymer composites: A review. *Composites Part C: Open Access*, 100269.

Saputra, A. (2020). *Pengaruh Quenching Pada Temperatur 850^{o}c Dengan Holding Time 15 Menit Terhadap Properti Material White Cast Iron Yang Diaplikasikan Kepada Grinding Ball Pada Ball Mill Untuk Produksi Semen*. Institut Teknologi Nasional Bandung.

Sari, M., Siswati, T., Suparto, A. A., Ambarsari, I. F., Azizah, N., Safitri, W., & Hasanah, N. (2022). *Metodologi penelitian*. Global Eksekutif Teknologi.

Sayed, A. R., Gupta, R., & Barai, R. (2019). Experimental investigation of C45 (AISI 1045) weldments using SMAW and GMAW. *AIP Conference Proceedings*, *2148*(1), 30047.

Sugestian, M. R. (2019). *Analisa Kekuatan Sambungan Las Smaw Vertical Horizontal Down Hand Pada Plate Baja Jis 3131sphc Dan Stainless Steel 201 Dengan Aplikasi Penyangga Piles Transfer Di Mesin Thermoforming (Stacking Unit)*. Institut Teknologi Nasional Malang.

Sugiyono. (2019). *Metode Penelitian Kuantitatif, Kualitatif, dan R&D*. Bandung : Alphabeta.

Wardani, I. P., Setyowati, V. A., Suheni, S., & Samudra, I. P. (2020). The Effect of Welding Current on Aisi 1045 Strength and Corrosion Rate. *Journal of Applied Sciences, Management, and Engineering Technology*, *1*(2), 40–45.